**DIRECTION DES ÉTUDES ET RECHERCHES**
SERVICE RÉACTEURS NUCLÉAIRES ET ECHANGEURS
DÉPARTEMENT MÉCANIQUE ET TECHNOLOGIE DES COMPOSANTS

EDF
Electricité de France



Octobre 1996

MOINEREAU D.

# L'EFFET PETIT DEFAUT ET L'APPROCHE LOCALE DE LA RUPTURE PAR CLIVAGE

# *THE SHALLOW FLAW EFFECT AND THE LOCAL APPROACH TO CLEAVAGE FRACTURE*

Pages : 15

97NB00048

**Diffusion :** J.-M. Lecœuvre
EDF-DER
Service IPN. Département PROVAL
1, avenue du Général-de-Gaulle
92141 Clamart Cedex



ISSN 1161-0611

**SYNTHÈSE :**

Cette note montre l'aptitude de l'approche locale de la rupture par clivage (modèle Beremin) à expliquer qualitativement les effets "petits défauts" dans le domaine du clivage.

De nombreux calculs élastoplastiques bidimensionnels ont été réalisés sur des éprouvettes fissurées soumises à des chargements thermique ou mécanique. Le comportement des éprouvettes a été examiné au moyen des courbes contrainte de Weibull $\sigma_w$ - facteur d'intensité de contrainte KJ.

Des différences importantes de comportement sont notées, liées au rapport a/w (profondeur relative des défauts étudiés). Pour un même niveau du facteur d'intensité de contrainte KJ, l'application du modèle de Weibull montre une probabilité de rupture par clivage plus élevée sur les éprouvettes comportant des défauts profonds.

**EXECUTIVE SUMMARY :**

The purpose of this paper is to evaluate the capability of local approach (Beremin model developed in the past by Ecole des Mines de Paris) to explain the shallow flaw effect in cleavage fracture, i.e. significantly higher toughness in specimens with short cracks compared to classical specimens with deep cracks. Numerous two-dimensional finite element calculations are performed on several cracked specimens (cladded and uncladded specimens with different values of a/W ratio) submitted to mechanical or thermal loading. The behavior of different specimens is examinated using the Weibull stress $\sigma_w$ versus stress intensity factor $K_J$ curves.

The comparison between different specimens shows significant differences, related to the a/W ratio. For a given level of the applied stress intensity factor, the probability of cleavage fracture evaluated with the Beremin model is higher on specimens containing deeper cracks. That means that, for a same probability of failure, higher fracture toughness must be obtained on specimens with shallow flaws.

This comparaison is completed by examinating the evolution of stress fields and plastic zones at the crack tip during the loading. Significant differences are observed between each specimen. Those differences are well correlated with the a/W ratio.

The effect of a/W ratio on the probability of cleavage fracture is underlined. These results can explain the increase of fracture toughness experimentally observed in different laboratories on specimens with shallow flaws.

# THE SHALLOW FLAW EFFECT AND THE LOCAL APPROACH TO CLEAVAGE FRACTURE

**D. MOINEREAU**
Electricité de France
Département Mécanique et Technologie des Composants
Les Renardières
77250 Moret-sur-Loing, FRANCE

## 1 - INTRODUCTION

It is now well known that specimens with short cracks can present significant higher fracture toughness compared to classical specimens with deep cracks ("shallow flaw effect"). Those effects have been experimentally observed by numerous laboratories. The local approach to cleavage fracture (Beremin model or Weibull model) has been developed in the past in France by F. Mudry at Ecole des Mines de Paris. This approach allows to evaluate the probability of cleavage fracture of a component submitted to thermal or mechanical loading.

~~The purpose of this paper is to evaluate~~ the capability of Beremin model to explain the shallow flaw effect in cleavage fracture. Numerous two-dimensional finite element calculations are performed on several cracked specimens (cladded and uncladded specimens with different values of a/W ratio) submitted to mechanical or thermal loading. The behavior of different specimens is examined using the Weibull stress $\sigma_w$ versus stress intensity factor $K_J$ curves. The stress fields and plastic zones at the crack tip are also compared on respective cracked specimens.

## 2 - THE LOCAL APPROACH TO CLEAVAGE FRACTURE AND ITS APPLICATION ON A CT SPECIMEN

### 2.1 The local approach to cleavage fracture

The local approach to cleavage fracture (Weibull model or Beremin model) is based on the elastic-plastic computation of the structure and on the use of a damage criterion which can be computed from the history of stress and strain in an elementary material cell [1] [2] [3]. The size of this elementary cell is a material parameter, related to the material microstructure.

The probability P of initiating cleavage fracture is expressed as:

$$P = 1 - \exp\left(-(\sigma_w/\sigma_u)^m\right)$$

$\sigma_w$ is the "Weibull stress" and characterizes the mechanical action exerted at the crack tip relevant to the risk of initiating cleavage fracture. This parameter is defined as:

$$\sigma_W = \left(\Sigma\, j_p\ \sigma_{1j}^{\,m}\ (V_j/V_0)\right)^{(1/m)}$$

$\sigma_{1j}$ is the value of maximum principal stress in the finite element cell, number j
$V_j$ is the volume of the mesh element
$V_0$ is the volume of the material cell ($V_0 = (50\ \mu m)^3$)

The numerical integration of the equation is made only in the elements which are plastically deformed (symbol $j_p$).

$\sigma_u$ and **m** are the parameters of this local criterion. $\sigma_u$ is defined as the intrinsic cleavage stress of the material (A508 Cl 3 steel) and characterizes the resistance to cleavage fracture. **m** is the Weibull parameter and characterizes the scatter in cleavage fracture. Both parameters, characteristics of the material, are supposed to be independent of temperature and can be determined using tensile testing of axisymmetric notched tensile specimens and numerical calculations.

### 2.2 Application of local approach to cleavage fracture to a CT specimen

In order to examine the sensitivity of the Weibull model to numerical aspects (mesh refinement at the crack tip, Weibull stress $\sigma_w$ calculation method), a two-dimensional numerical analysis is conducted on a classical CT 50 specimen (net thickness: 50 mm, a/W: 0.55, material: A508 Cl3 ferritic steel).

The elastic-plastic analysis of the specimen is performed using the SYSWELD finite element program developed by Framatome (plane strain assumption). Several meshes are considered with different mesh refinements at the crack tip: square elements of 25 μm by 25 μm, 50 μm by 50 μm, 200 μm by 200 μm and 400 μm by 400 μm. The mechanical properties of the A508 Cl3 ferritic steel taken into account are those used in the interpretation of cladded beam tests (§ 3).

After the elastic-plastic calculation of the CT specimen, the stress intensity factor $K_J$ (deduced from the computation of J integral by the following expression $K_J = (E.J/1\text{-}v^2)^{0.5}$ ) and the Weibull stress $\sigma_w$ are computed using specific post-processors of SYSWELD program. Two methods are used for the computation of the Weibull stress $\sigma_w$, «partielle gauss method» and «partielle method», whether you consider stresses at the Gauss points (first method) or average stresses in the element (second method). The Weibull model parameter m considered in this study is the value usually used by Framatome in safety analyses (m = 22, [4]).

The main results are presented on figures 1 (stress intensity factor $K_J$ versus load) and 2 (Weibull stress $\sigma_w$ versus stress intensity factor $K_J$). Figure 1 confirms of course the fact that the stress intensity factor $K_J$ is not mesh dependent (same results obtained on the four meshes).

Figure 2 shows that the local approach to cleavage fracture can be very sensitive to numerical aspects. First, the Weibull stress $\sigma_w$ is dependent on the calculation method whether you consider in this type of analysis stresses at Gauss points or average stresses inside the elements. Higher values of Weibull stress are obtained in the first case because the averaging procedure decreases the peak stress recorded in each element. Secondly, the results can be very dependent on the mesh size if it is not sufficiently refined. Considering those results, we show that the use of 50 μm square elements at the crack tip is sufficient since results are similar with 25 μm or 50 μm square elements. On the contrary, the use of larger elements (200 μm or 400 μm) at the crack tip is not sufficient. In this case, the Weibull stress $\sigma_W$ (and consequently the probability of cleavage fracture) is strongly underestimated.

## 3 - RESULTS OBTAINED ON CLADDED BEAMS UNDER BENDING

### 3.1 A few words about the experimental program

In France, the safety analyses regarding the risk of fast fracture in the reactor pressure vessels are usually performed with elastic and elastic-plastic calculations taking into account the effect of stainless steel cladding and residual stresses [4]. Electricité de France has conducted in the past a large research program including cleavage fracture tests on cladded mock-ups, in order to validate several structural integrity analysis methods [5] [6] [7]. Cleavage fracture has been obtained at about -170°C on four cladded mock-ups each containing a shallow subclad flaw.

Most of the details of this research programme, with numerical interpretations using a classical approach, have been already presented in papers [5] [6] [7]. Main characteristics of this programme are summarized in this section before presenting the interpretation using local approach to cleavage fracture.

#### *Mock-ups*

Four cladded beams, referenced DSR4, DSR1, DSR3, DD2 and each containing an underclad crack, have been submitted to a four-point bending mechanical loading. The central part of mock-ups is extracted from a vessel shell ring of forging A508 Cl3 ferritic steel ($RT_{NDT}$ = -40°C). The size of the specimens is approximately 120 mm thickness, 1700 mm length and 150 mm width. The cladding is made with two layers on the top surface using an automatic submerged-arc welding process, a first layer in 309L austenitic stainless steel and the second in 308L stainless steel. After cladding, a stress relief heat treatment is applied at 600°C for 8 hours. The artificial underclad crack is made before cladding by machining and fatigue.

#### *Testing conditions*

The specimens are loaded in four-point bending at very low temperature (about -170°C) to obtain crack instability in base metal by cleavage fracture. At this temperature, the material mechanical properties (yield strength) can be considered as representative of the end of life vessel material properties.

#### *Materials characterization*

Characterization of stainless steel cladding, base metal and heat-affected zone is performed including chemical analyses, Charpy impact tests, tensile tests, crack-growth resistance and fracture toughness.

#### *Identification of Weibull model parameters m, $\sigma_u$*

The identification of Weibull model parameters m and $\sigma_u$ is performed on axisymmetrically notched tensile specimens AE2 (notch radius 2 mm). The procedure used for this has been previously described in references [1] [2]. This identification is conducted in the framework of a cooperative research program between Electricité de France, CEA, Framatome and AEA Technology. The material is taken from a forging vessel ring of A508 Cl3 ferritic steel, as for the cladded specimens previously described.

Forty tests on axisymmetric notched tensile specimens are performed at -170°C in the pure cleavage regime, conducted by two laboratories. Two sets of parameters are finally identified, depending the number of notched specimens taken into acccount in the identification procedure:

. m = 27, $\sigma_u$ = 2657 MPa (20 specimens)

. m = 24, $\sigma_u$ = 2696 MPa (40 specimens).

#### *Experimental results*

A cleavage fracture has been obtained on each cladded specimen, without crack arrest. The main characteristics of mock-ups and flaws are summarized in table 1.

### 3.2 Interpretation of cladded beam tests with local approach to cleavage fracture

The interpretation of cladded mock-up tests is conducted using two-dimensional finite element computations (with plane strain assumption) performed with the SYSWELD finite element program. After the elastic-plastic calculations, the probability of failure of the mock-ups during the test is evaluated with the Weibull model using parameters m, $\sigma_u$ previously determined. The mesh refinement at the crack tip is the same as in the CT specimen analysis (square elements of 50 µm by 50 µm).

Some of the results are shown in figure 3 (using option «partielle gauss» in Weibull stress $\sigma_w$ calculation). The calculated probability of failure is in each case in agreement with the experimental result (cleavage failure of the specimen). This probability is also very similar whether you consider m, $\sigma_u$ parameters identified on 20 specimens (m = 27, $\sigma_u$ = 2657 MPa) or 40 specimens (m = 24, $\sigma_u$ = 2696 MPa).

The sensitivity of results (probability of failure) to mesh refinement and Weibull stress calculation method is presented in analysis of DD2 mock-up in figure 4. This test is interpreted using a very refined mesh (50 µm by 50 µm square elements) and additional meshes with larger square elements (200 µm by 200 µm and 400 µm by 400 µm). The effects of mesh refinement (size of elements at the crack tip) and Weibull stress $\sigma_w$ calculation (stress at the gauss points or average stress in the element) are clearly underlined on this figure, as in the case of the CT specimen. The use of too coarse finite element meshes leads to strongly underestimate the final probability of failure.

### 3.3 Comparison between cladded beams and CT specimen

The CT specimen is compared to cladded mock-ups using Weibull stress $\sigma_W$ versus stress intensity factor $K_J$ curves. As the Weibull stress $\sigma_W$ is very mesh size dependent, the same mesh refinement at the crack tip is required in different specimens. A first comparison is made using square elements of 50 µm * 50 µm at the crack tip, a second comparison is made with larger square elements (200 µm * 200 µm).

These comparisons are presented on figure 5. It shows that the Weibull stress $\sigma_W$ in the CT specimen and in several cladded mock-ups, similar for low values of the applied stress intensity factor $K_J$, are very different for higher values of $K_J$ (30 MPa.m$^{0.5}$ and over). It means that the probability of cleavage fracture evaluated with this model (Weibull model or Beremin model) can be different between a CT specimen and a cladded mock-up although the applied stress intensity factors in the different structures are identical. For a given level of applied stress intensity factor $K_J$, the higher probability of failure (or the higher Weibull stress $\sigma_w$) is obtained on the specimen containing the deeper crack (CT specimen with a/W = 0.55). Furthermore, other significant differences are observed between CT specimen and cladded specimens containing short underclad crack for a given level of the stress intensity factor: decreasing opening stress on the cracked ligament and increasing of the plastic zone size for the specimens with short crack. This aspect will be discussed in more detail in the following paragraph.

These results suggest a shallow flaw effect (increasing of fracture toughness on specimens with short cracks) due to very different values of a/W ratio between CT specimen (a/W = 0.55) and cladded specimens (0.033 < a/W < 0.108) [8] [9] [10].

## 4 - THE SHALLOW FLAW EFFECT

Previous comparison between a CT specimen (a/W = 0.55) and cladded mock-ups (low values of a/W) has shown significant differences on the probability of cleavage fracture (evaluated with the Weibull model) of these specimens for the same level of the applied stress intensity factor. As it has been mentionned before, a shallow flaw effect is suggested. A parametric study, including numerous two-dimensional finite element computations on cracked specimens, has been conducted to confirm or infirm this effect.

Several geometrical configurations are taken into account in this study:

- CT specimen with a/W = 0.55
- Four point-bending cracked specimens with the following values of a/W: 0.55, 0.2 and 0.05 (W = 100 mm in each case)
- Four point-bending cladded specimen (cladding thichness 7 mm) containing an underclad crack (a/W = 0.05, total thickness 107 mm)
- Cladded specimens presented previously in this paper, containing an underclad crack (DSR4, DSR1, DSR3 and DD2 with 0.033 < a/W < 0.108).

The mesh refinement at the crack tip is identical for each specimen (square elements of 50 µm by 50 µm, as it can be seen on figure 6). The elastic-plastic computation of each specimen is conducted with the SYSWELD finite element program (plane strain assumption, small scale yielding condition). The stress-strain curve used in the computations is the curve determined at -170°C on the A508 Cl3 ferritic steel of cladded mock-ups (yield strength: 768 MPa, Young modulus: 210000 MPa). The Weibull parameter m taken into account for the calculation of the Weibull stress $\sigma_w$ is m = 22.

The comparison between different specimens is made on figure 7 using Weibull stress $\sigma_w$ versus stress intensity factor $K_J$ curves ($K_J$ is deduced from the elastic-plastic computation of J integral). The effect of a/W ratio on $\sigma_w$ versus $K_J$ curves is clear. The main observations previously exposed during the comparison between a CT specimen and cladded specimens are confirmed. The Weibull stress $\sigma_w$ , similar for very low values of the stress intensity factor, differs markedly in different specimens as soon as the loading (and plasticity in base metal) increases. The evolution is perfectly correlated with a/W ratio: for a given level of the stress intensity factor, higher values of Weibull stress (consequently higher values of the probability of cleavage fracture) are obtained in specimens containing deeper cracks. These observations confirm the shallow flaw effect previously suggested in the comparison between a CT specimen and cladded mock-ups. That means that, for a same probability of failure, higher cleavage toughness is obtained on specimens containing short cracks (loss of constraint).

The comparison between different cracked specimens is completed by examinating the evolution of stress fields and plastic zones at the crack tip during the loading. Significant differences are observed between each specimen, as it can be seen on figures 8 (evolution of $\sigma_x$ and $\sigma_y$ stresses on the ligament) and 9 (plastic zone at the crack tip) for different values of the applied stress intensity factor $K_J$. For a same level of loading ($K_J$), we notice a decrease of stresses $\sigma_x$ (parallel to crack) and $\sigma_y$ (opening stress) on the ligament at the crack tip and a marked increase of the plastic zone size in specimens with shallow crack.

This parametric study confirms some results on constraint effect obtained by AEA Technology with local approach to cleavage fracture [11].

## 5 - COMPLEMENTARY RESULTS ON CLADDED VESSELS UNDER THERMAL LOADING

A cooperative research programme involving EDF, CEA, Framatome and AEA Technology is in progress in the field of the local approach to cleavage fracture. Within the framework of this collaboration, numerous two-dimensional finite element computations have been performed by partners on specimens and structures under mechanical or thermal loading [12].

Among different analyses conducted, the behavior of two cladded vessels submitted to thermal transient has been studied using local approch to cleavage fracture. Results are presented in detail in paper [12]. Main results obtained by EDF on these structures are summarized in this section, including a comparison with a CT specimen [12].

### 5.1 Cladded vessels geometry

Two cladded vessels with small underclad crack are considered, differing only by the underclad crack size (figure 10). The base metal is a A508 Cl3 forging steel and the cladding is a classical A309L - A308L stainless steel. The main dimensions are the following:

| | |
|---|---|
| . internal radius | Ri: 2000 mm |
| . external radius | Re: 2207 mm |
| . cladding thickness | 7 mm |
| . base metal thickness | 200 mm |
| . subclad flaw | 6.2 mm (first vessel) |
| | 12.2 mm (second vessel) |

The crack taken into account in both cases is an axisymmetrically subclad flaw, including a 0.2 mm tip in cladding in order to calculate the stress intensity factor $K_J$ at the crack tip in cladding.

### 5.2 Material properties, loading and finite element models

The materials properties taken into account in this work are described in paper [12]. The thermal properties and the thermal expansion coefficients are temperature dependent, the other mechanical properties are not temperature dependent (Young's modulus, yield strength, Poisson ratio and stress-strain curves). The stress-strain curves used in the computations are shown in figure 11.

Each vessel is submitted to a thermal transient applied on the inner cladded vessel (figure 12), without pressure. The thermal exchange coefficient is fixed to 5000 $W/m^2.°C$ on the inner surface (AB ligament on figure 10) and is nil on the other surfaces.

As the use of Beremin model requires a great care in the mesh refinement, the refined zone at the crack tip in base metal is constituted of 50 µm by 50 µm square elements for both cladded vessels. This refinement is very similar to mesh refinement used in the analyses described in section 4 of this paper.

### 5.3 Elastic-plastic analyses

The two-dimensional elastic-plastic analyses are conducted with the ASTER finite element programme (developed by EDF). All the results are presented in paper [12]. Figure 13 shows the evolution of the stress intensity factor $K_J$ in base metal during the transient.

The analysis of a CT specimen is conducted in parallelel, using same mechanical properties as base metal of cladded vessels. The mesh refinement of the CT specimen at the crack tip is of course the same as cladded vessels (square elements of 50 µm by 50 µm). Figure 14 shows the corresponding Weibull stress $\sigma_w$ versus stress intensity factor $K_J$ curve.

### 5.4 Comparison with a CT specimen

Figure 15 shows the comparison between CT specimen and cladded vessels, using the Weibull stress versus stress intensity factor curves. This figure confirms the fact that the $\sigma_w$ - $K_J$ curves are very dependent on the specimen geometry, more particularly the «a/W» ratio (0.55 for the CT specimen, ≈ 0.06 for the vessel with a 12.2 mm subclad flaw, ≈ 0.03 for the vessel with a 6.2 mm subclad flaw). As in the case of previous calculations presented in section 4 of this paper, the application of local approach to cleavage fracture (Beremin model) leads to higher probability of cleavage failure (higher Weibull stress) on specimen with deeper crack (CT specimen) for a given applied stress intensity factor $K_J$ in base metal. These results obtained with thermal loading confirm numerical results previously obtained on cracked specimens under mechanical loading.

## 6 - CONCLUSION

The capability of the local approach to cleavage fracture (Beremin model) to explain the shallow flaw effect experimentally observed in cleavage fracture has been investigated in this paper. Numerous two-dimensional finite element elastic-plastic computations have been performed on several cracked specimens submitted to mechanical and thermal loading. The behavior of respective cracked specimens has been examined and compared using the Weibull stress $\sigma_w$ versus stress intensity factor $K_J$ curves.

Significant differences have been observed related to the «a/W» ratio. The application of Beremin model shows higher probability of cleavage failure on specimens with deeper cracks for a given level of the stress intensity factor.

The local approach to cleavage fracture can explain the increase of fracture toughness experimentally observed by numerous laboratories on specimens with shallow flaws (shallow flaw effect).

## ACKNOWLEDGMENTS

Some of the results presented in this paper have been obtained in the framework of a cooperative action between EDF, CEA, Framatome and AEA Technology. The author would like to thank Mrs Brochard (CEA), MM. Guichard, Bhandari and Pellissier Tanon (Framatome), Mr Sherry and Mrs France (AEA Technology) for helpful discussions.

## REFERENCES

[1] Mudry F., "Etude de la rupture ductile et de la rupture par clivage d'aciers faiblement alliés" - Thesis of Doctorat d'Etat at Ecole des Mines de Paris, 1982.

[2] Mudry F., "A local approach to cleavage fracture" - International Seminar on Local Approach of Fracture - Proceedings pp 165-186 - Les Renardières, June 3-5, 1986.

[3] Pellissier-Tanon A., Devaux J.C. and Houssin B., "Application of statistical cleavage criteria to fracture control of pressure vessels" - ECF 6 Conference - Vol. 2 pp. 903-918, EMAS, 1986.

[4] Pellissier-Tanon A., Grandemange J., Houssin B. and Buchalet C., "French experience on the verification of pressurized water reactor vessels integrity", EPRI Research project 2975-2, 1989.

[5] Moinereau D., Bethmont M., Chas G. and Rousselier G., "Cleavage fracture of plates with small underclad crack: Experiments presentation and interpretation by fracture mechanics" - Pressure Vessel and Piping Conference - Vol. 213 pp 53-59 - San Diego, June 23-27, 1991.

[6] Moinereau D., Rousselier G. and Bethmont M., "Behavior of underclad cracks in reactor pressure vessels: evaluation of mechanical analyses used in french RPV integrity assessment by cleavage fracture tests on large scale plates" - Pressure Vessel and Piping Conference - Vol. 250 pp 44-59 - Denver, July 25-29, 1993.

[7] Moinereau D., Rousselier G., "The analysis of underclad cracks in large-scale tests using the local approach to cleavage fracture" - ASTM, 27th National Symposium on Fatigue and Fracture Mechanics - Williamsburg, June 26-29, 1995.

[8] Theiss T.J., Rolfe S.T. and Shum D.K., "Shallow-crack toughness results for reactor pressure vessel steel", International Conference Shallow Crack Fracture Mechanics, Toughness Tests and Applications, Cambridge, 1992.

[9] Smith J.A. and Rolfe S.T., "The effect of crack depth (a) and crack depth to width ratio (a/W) on the fracture toughness of A533-B steel" - Pressure Vessel and Piping Conference - Vol. 250 pp 247-255 - Denver, July 25-29, 1993.

[10] Tigges D., Piques R., Frund J.M. and Pineau A., "Shallow crack effect on fracture toughness in a low alloy steel" - ECF 10 Conference - Vol. 1 pp 637-646, 1994.

[11] Sherry A.H., Sanderson D.J., Lidbury D.P.G., Ainsworth R.A. and Kikuchi K., "The application of local approach to assess the influence of in-plane constraint on cleavage fracture" - Pressure Vessels and Piping Conference - Hawaï, July 24-27, 1995.

[12] Moinereau D., Brochard J., Guichard D., Bhandari S., Sherry A. and France C., "Local approach of cleavage fracture applied to a vessel with subclad flaw. A benchmark on computational simulation" - Pressure Vessel and Piping - Montreal, July 22-25, 1996.

## TABLES AND FIGURES

TABLE 1: EXPERIMENTAL RESULTS ON CLADDED MOCK-UPS

| | DSR4 | DSR1 | DSR3 | DD2 |
|---|---|---|---|---|
| Width (mm) | 145 | 150 | 150 | 150 |
| Total thickness (mm) | 128 | 125 | 124.5 | 126 |
| Cladding thickness (mm) | 8 | 5 | 4.5 | 6 |
| Flaw depth (mm) | 5 | 4 | 13 | 4.5 |
| Flaw width (mm) | 50 | 50 | 40 | 50 |
| **Critical load (kN)** | 640 | 804 | 695 | 890 |

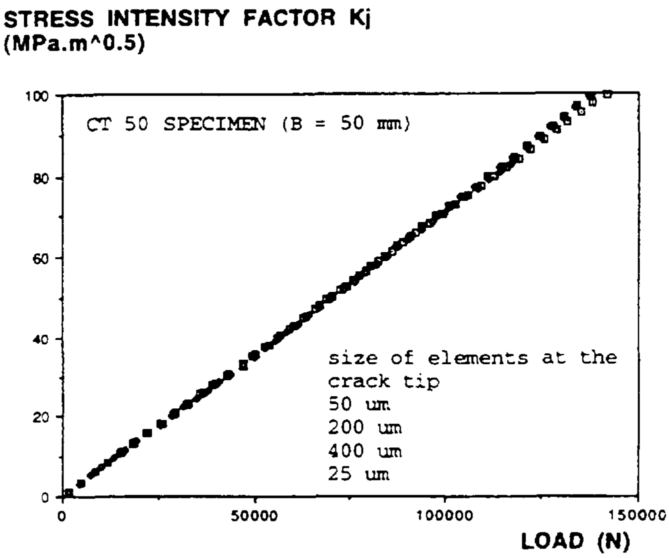


FIG 1. STRESS INTENSITY FACTOR $K_J$ VERSUS LOAD (CT SPECIMEN)

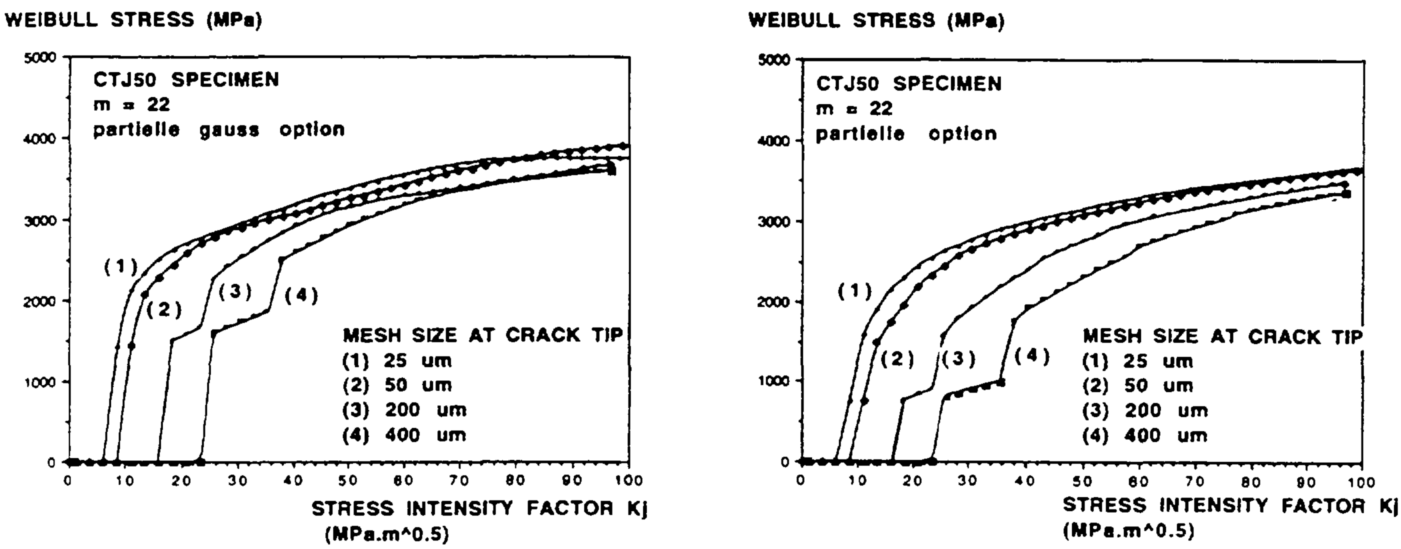


FIG 2. WEIBULL STRESS $\sigma_W$ VERSUS STRESS INTENSITY FACTOR $K_J$ (CT SPECIMEN)

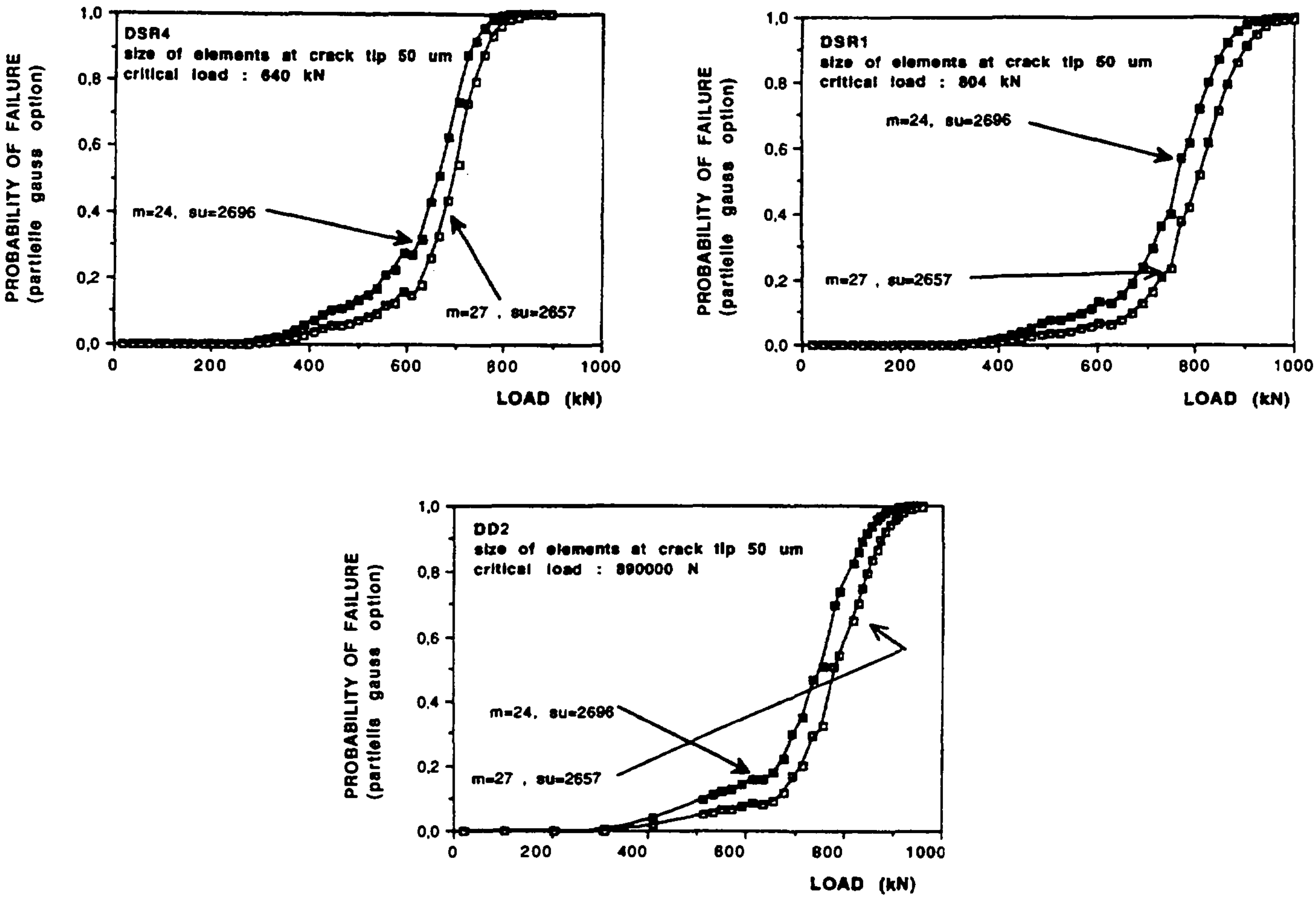


FIG 3. PROBABILITY OF FAILURE VERSUS LOAD FOR CLADDED MOCK-UPS DSR4, DSR1, DD2

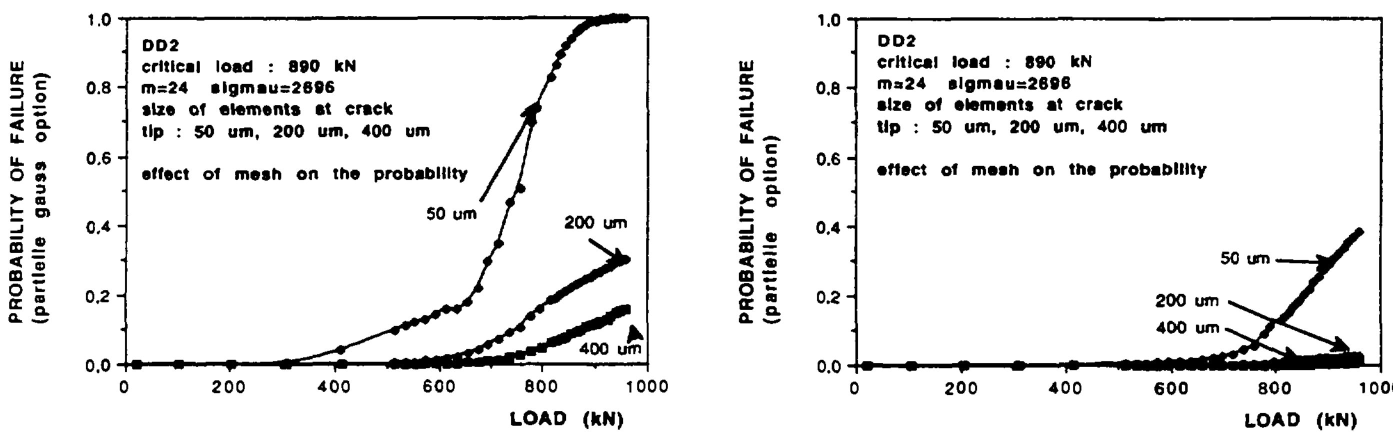


FIG 4. PROBABILITY OF FAILURE VERSUS LOAD CURVE FOR DD2 MOCK-UP.
SENSITIVITY OF RESULTS TO MESH REFINEMENT

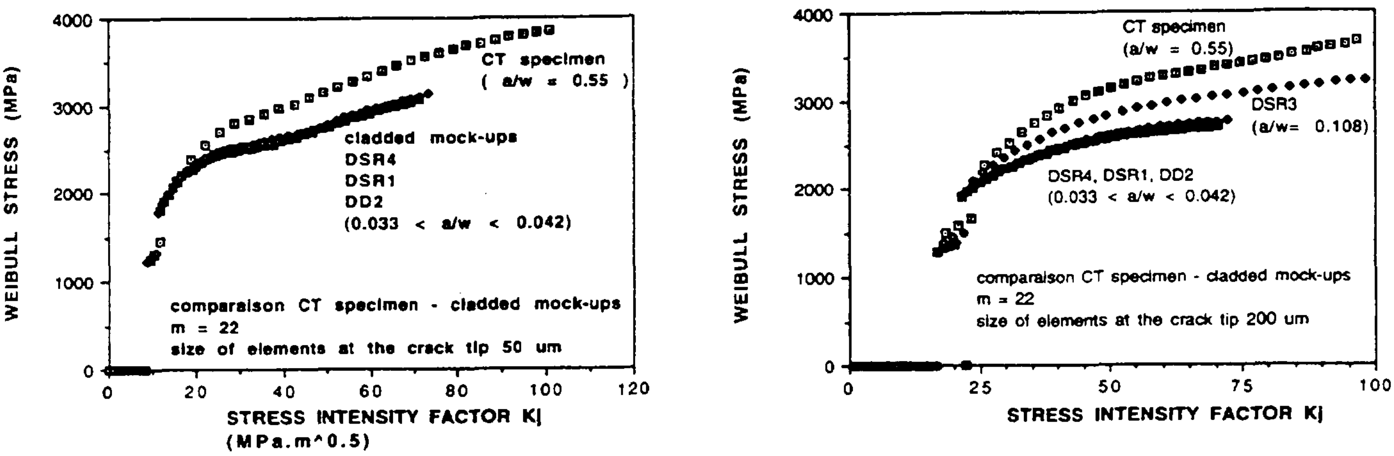


FIG 5. WEIBULL STRESS $\sigma_W$ VERSUS STRESS INTENSITY FACTOR $K_J$ CURVE.
COMPARISON BETWEEN CT SPECIMEN AND CLADDED MOCK-UPS

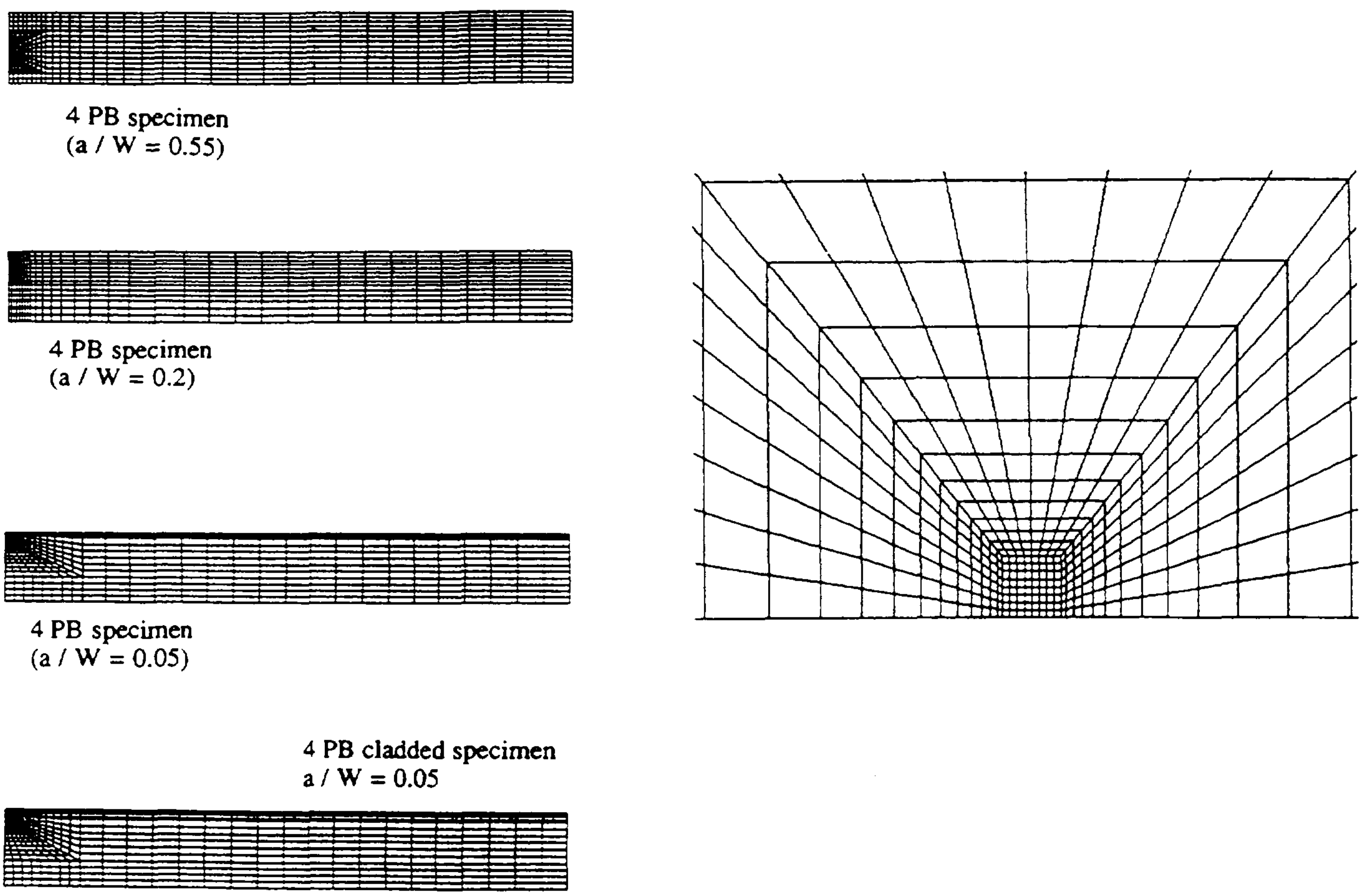


FIG 6. COMPARISON BETWEEN DIFFERENT CRACKED SPECIMENS.
MESH REFINEMENT AT THE CRACK TIP

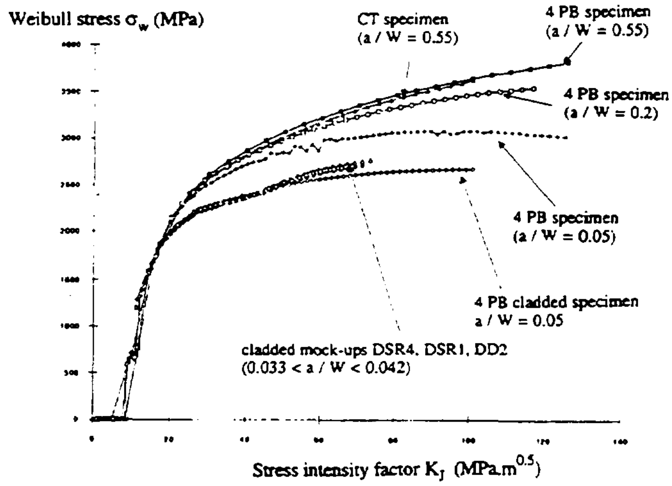


FIG 7. WEIBULL STRESS $\sigma_W$ VERSUS STRESS INTENSITY FACTOR $K_J$ CURVE. COMPARISON BETWEEN DIFFERENT CRACKED SPECIMENS

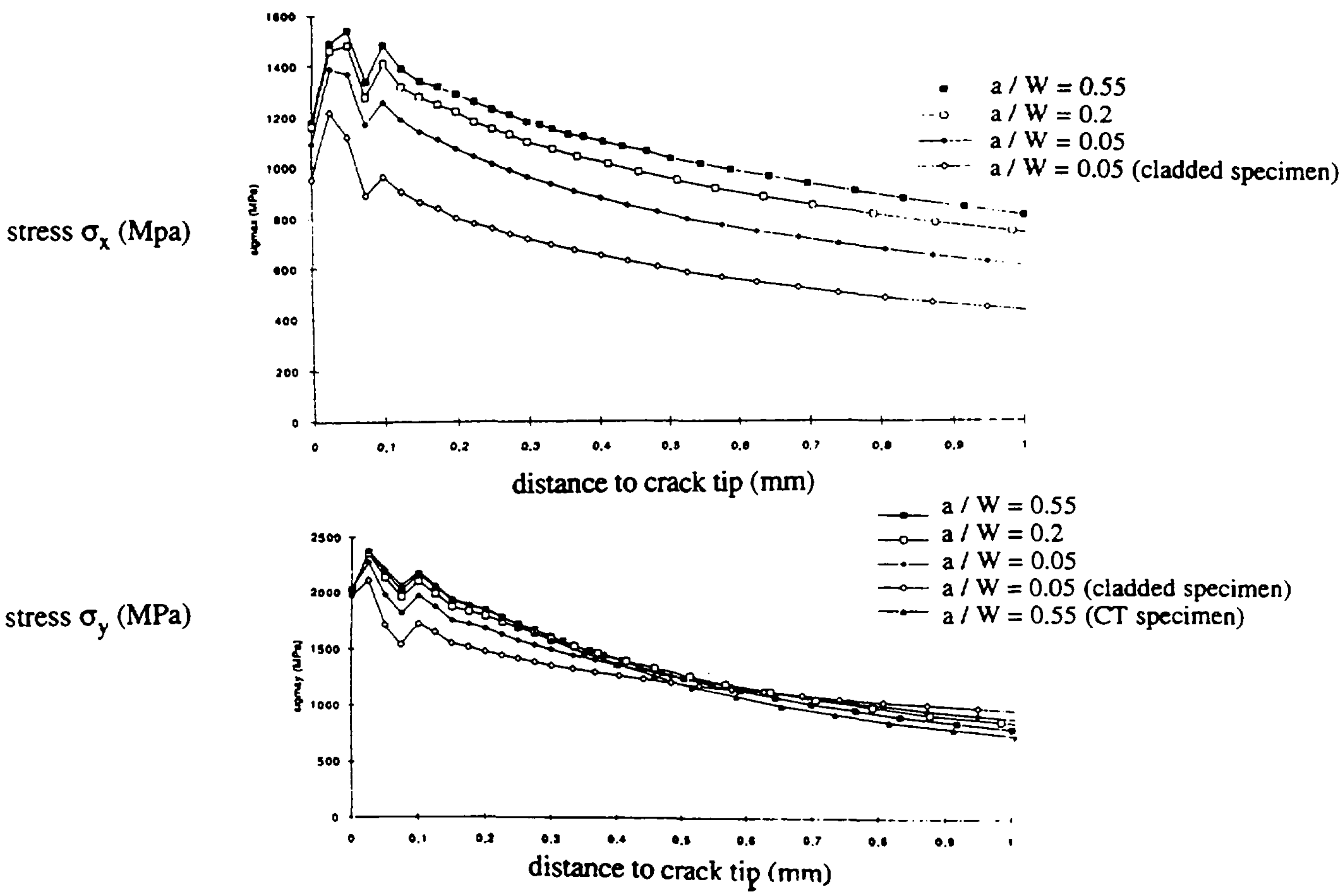


FIG 8. STRESS PROFILE ON LIGAMENT OF DIFFERENT CRACKED SPECIMENS ($K_J$ = 60 MPa.m$^{0.5}$ FOR EACH SPECIMEN)

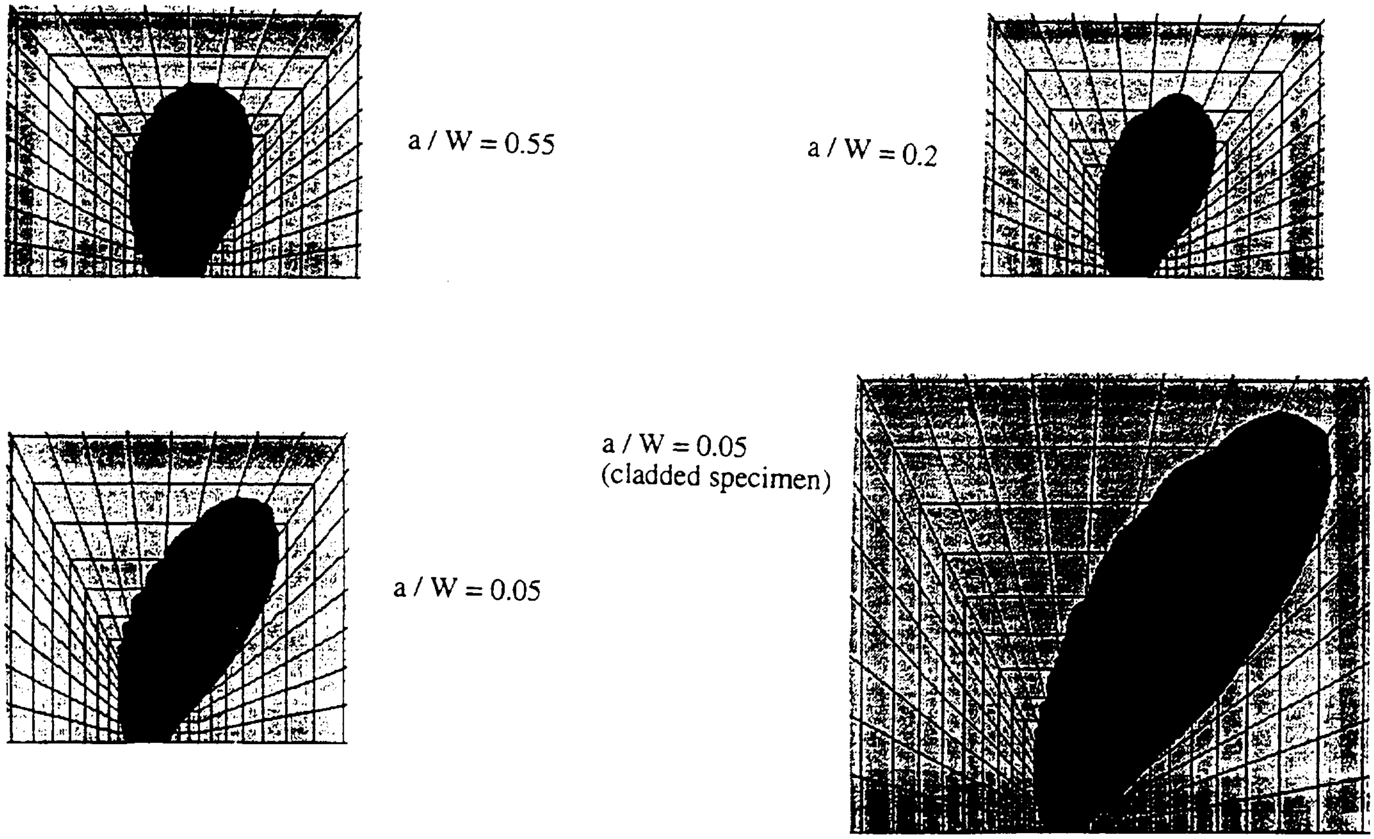


FIG 9. PLASTIC ZONE AT THE CRACK TIP. COMPARISON BETWEEN DIFFERENT CRACKED SPECIMENS ($K_J$ = 60 MPa.m$^{0.5}$ FOR EACH SPECIMEN)

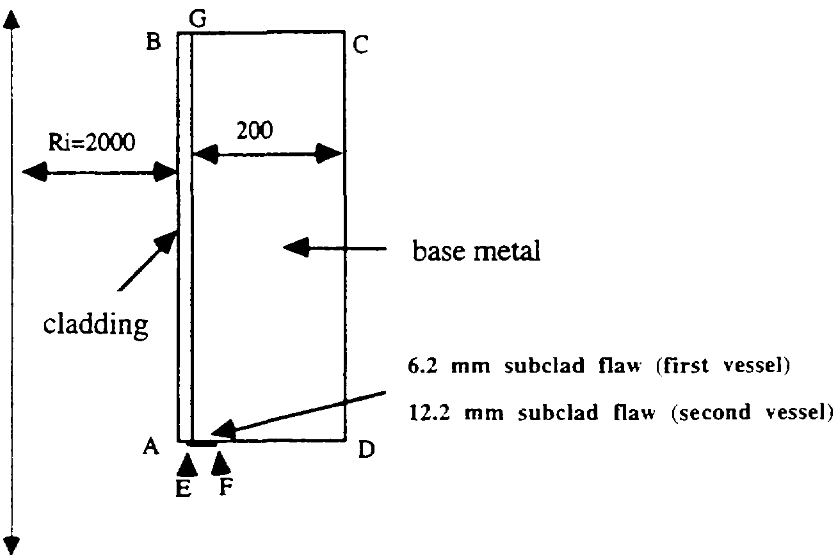


FIG 10. GEOMETRY OF THE CLADDED VESSELS

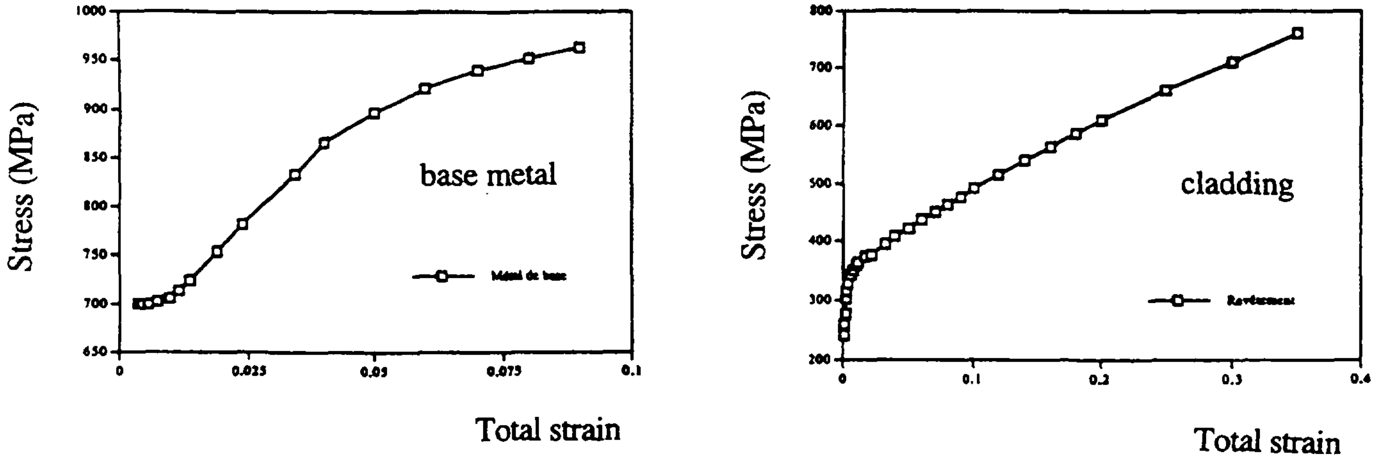


FIG 11. STRESS - STRAIN CURVES

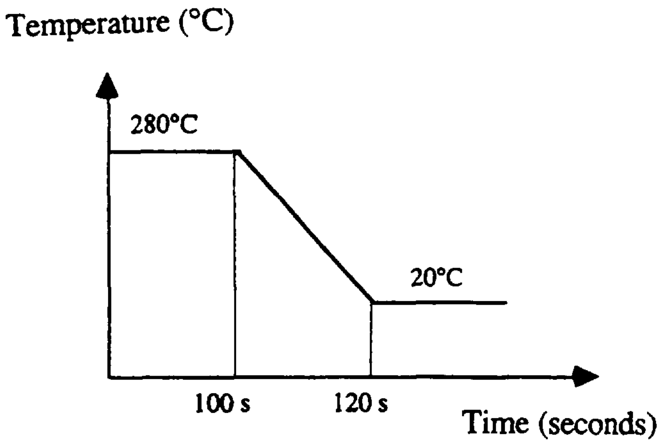


FIG 12. THERMAL TRANSIENT APPLIED TO THE VESSELS

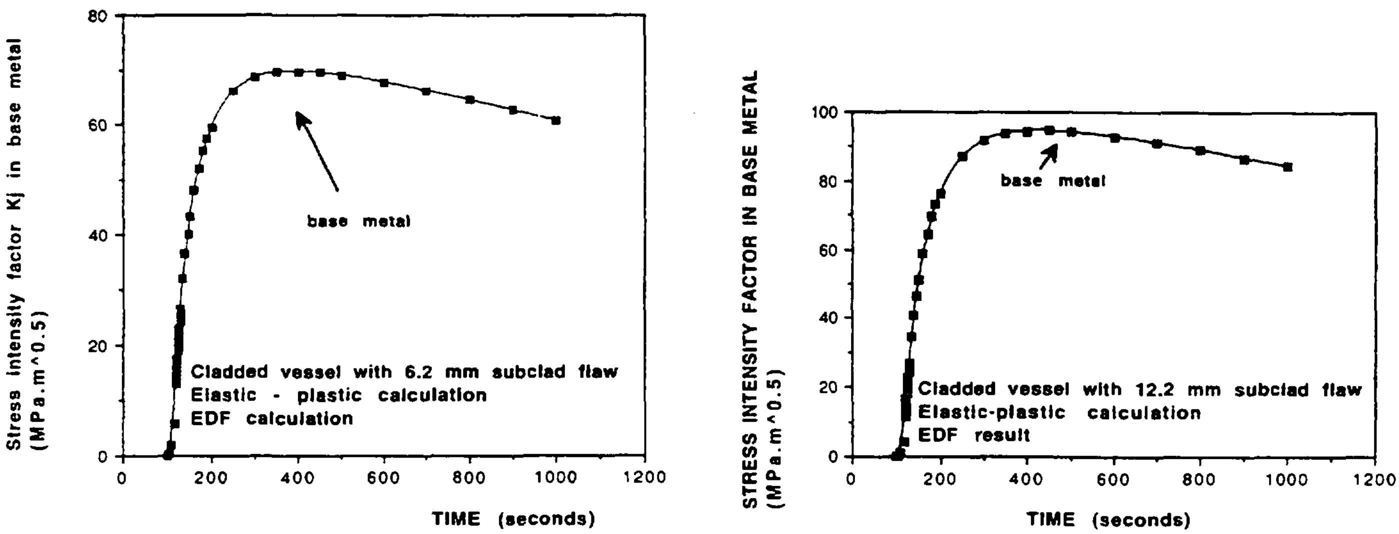


FIG 13. STRESS INTENSITY FACTOR $K_J$ IN BASE METAL DURING THE TRANSIENT

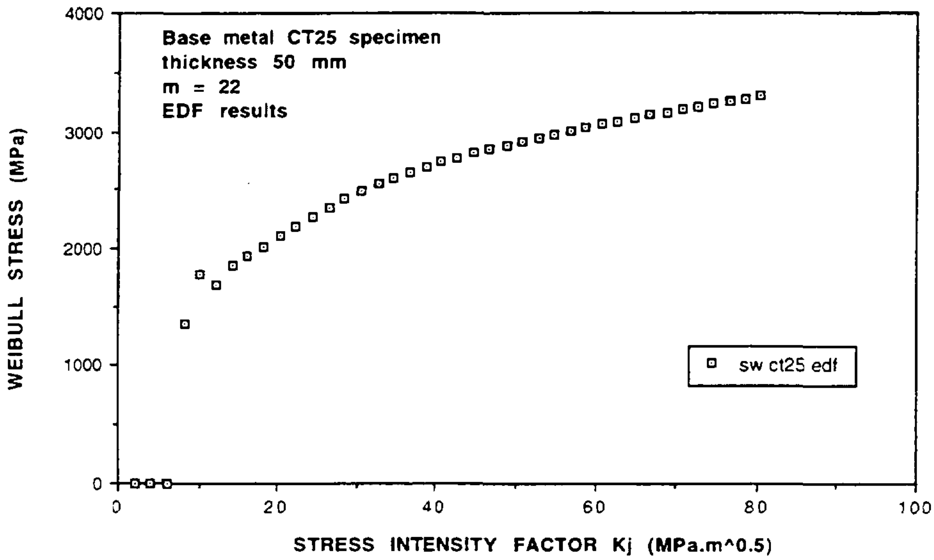


FIG 14. WEIBULL STRESS $\sigma_W$ VERSUS STRESS INTENSITY FACTOR $K_J$ (CT SPECIMEN)

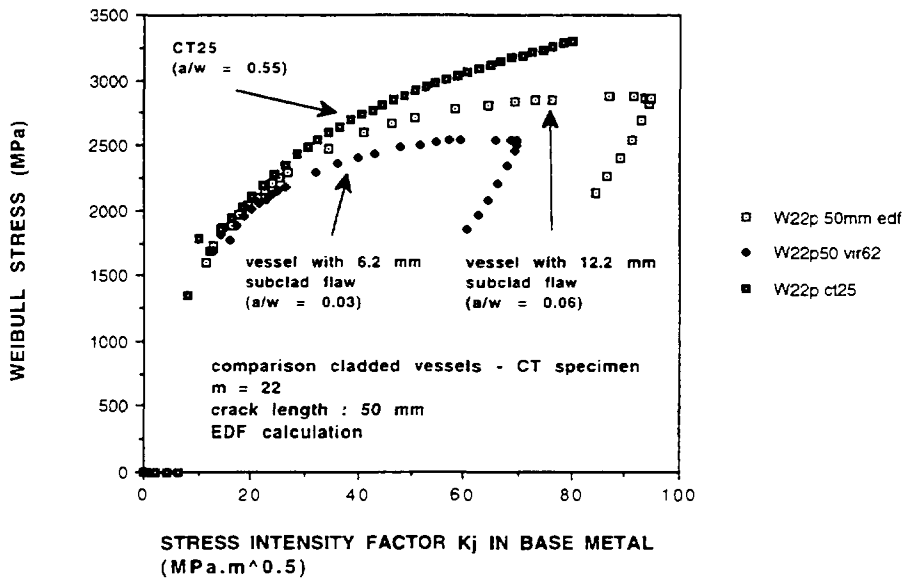


FIG 15. COMPARISON BETWEEN CLADDED VESSELS AND CT SPECIMEN USING BEREMIN MODEL ($\sigma_W$ VERSUS $K_J$ CURVE)

EDF

Electricité de France

DIRECTION DES ÉTUDES ET RECHERCHES

1, AVENUE DU GENERAL-DE-GAULLE - BP 408 - 92141 CLAMART CEDEX FRANCE - TÉL. 33 1 47 65 58 11 - FAX 33 1 47 65 49 27 - e.mail elisa.nuc@der.edfgdf.fr